How many molecules form a liquid?

1999 J. Phys.: Condens. Matter 11 A175

(http://iopscience.iop.org/0953-8984/11/10A/013)

J. Phys.: Condens. Matter **11** (1999) A175–A188. Printed in the UK PII: S0953-8984(99)00625-6

How many molecules form a liquid?

F Kremer†‖, A Huwe†, M Arndt†, P Behrens‡ and W Schwieger§¶

† University of Leipzig, Department of Physics, D-04103 Leipzig, Germany
‡ University of Hannover, Department of Chemistry, D-30167 Hannover, Germany
§ Department of Chemistry, Martin Luther University, Halle–Wittenberg, D-06108 Halle, Germany

Received 2 October 1998

Abstract. Broad-band dielectric spectroscopy (10^{-2} Hz–10^{9} Hz) is employed to study the molecular dynamics of (dielectrically active) glass-forming liquids which are confined to (dielectrically inactive) zeolites and nanoporous glasses. For the H-bond-forming liquid ethylene glycol (EG) embedded in zeolites of different sizes and topologies one observes a sharp transition from a single-molecule dynamics (with an Arrhenius-type temperature dependence) to that of a liquid (with a temperature dependence of the mean relaxation rate following a Vogel–Fulcher–Tammann (VFT) law): while EG in silicalite (showing a single-molecule relaxation) has a coordination number of four, EG in zeolite beta or $AlPO_4$-5 has a coordination number of five and behaves like a bulk liquid.

For the H-bonded liquid propylene glycol confined to (uncoated and silanized) nanopores (pore sizes: 2.5 nm, 5.0 nm and 7.5 nm), a molecular dynamics is observed which is comparable to that of the bulk liquid. Due to surface effects in uncoated nanopores, the relaxation time distribution is broadened on the long-term side and the mean relaxation rate is decreased by about half a decade. This effect can be counterbalanced by lubricating the inner surfaces of the pores. That causes the molecular dynamics of the molecules inside the pores to decouple from the solid walls and the resulting relaxation rate becomes slightly faster compared to that for the bulk liquid.

For the 'quasi'-van der Waals liquid salol confined to silanized nanopores, the molecular dynamics is completely different to that for the H-bonded systems: over a wide temperature range, the dynamics of the confined system is identical to that of the bulk liquid. But with decreasing temperature, a sharp pore-size-dependent transition is found from a VFT-type to an Arrhenius-type temperature dependence. This reflects the inherent length scale of cooperativity of the dynamic glass transition.

1. Introduction

It is a challenge to modern experimental physics to find out under what conditions an ensemble of a few molecules starts to behave like a liquid [1–7]. This question can be readily approached by measuring over a broad frequency range the molecular dynamics of guest molecules embedded in (zeolitic and nanoporous) host systems of well controlled confining geometry [6–9]. Modern solid-state chemistry enables the realization of the extreme of a single isolated molecule in one zeolitic cage by the use of structure-directed synthesis where the structure-directing agents (or templates) become occluded in specific voids during the process of growth of an inorganic framework. Varying the size and the topology of the zeolitic host system allows one to study in detail the transition from a single-molecule dynamics to

‖ Corresponding author.
¶ Present address: University Erlangen-Nürnberg, D-91058 Erlangen, Germany.

0953-8984/99/SA0175+14$19.50

that of a bulk liquid. It is evident that this problem is intimately related to the understanding of the cooperative dynamics and its inherent length scale in glass-forming liquids [4–8, 10–15].

2. Experimental procedure

Zeolites offer the unique possibility of varying the dimensionality and the topology of a spatial confinement on a sub-nanometre scale in a controlled manner. Silica sodalite consists of identical so-called β-cages, with free inner diameters of 0.6 nm. Ethylene gylcol (EG) is one of the structure-directing agents which control the formation of silica sodalite [16,17]. Exactly one EG molecule becomes occluded in one sodalite cage during synthesis and cannot escape from it unless the cage is thermally decomposed [17]. Silicalite-I, zeolite beta and $AlPO_4$-5

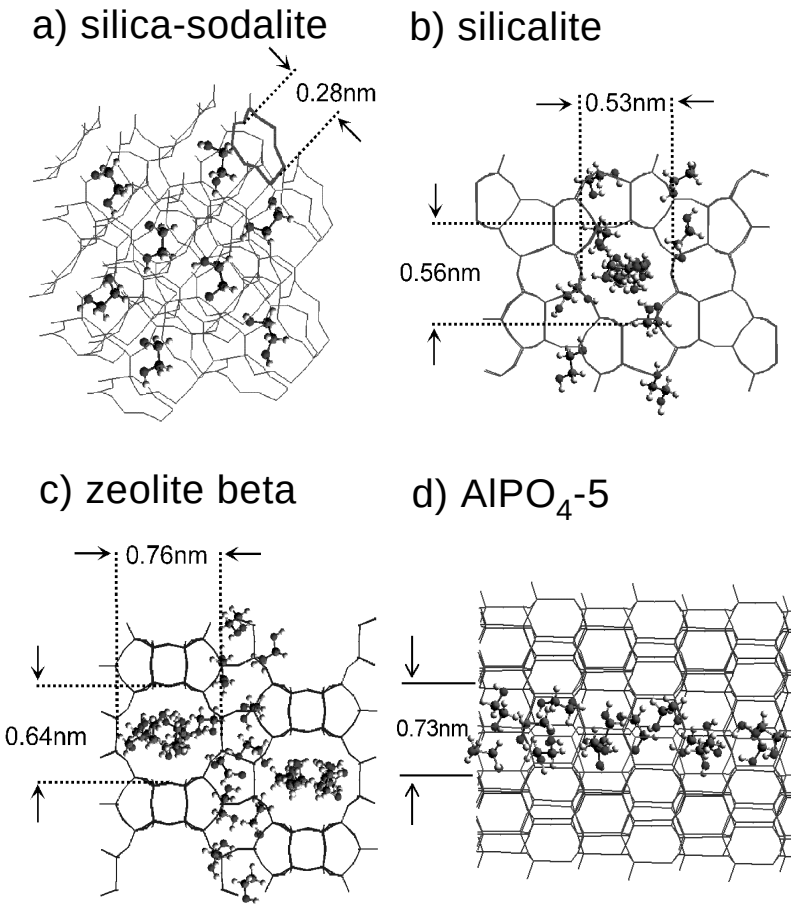

Figure 1. Schematic diagrams of the zeolitic host systems in which the guest molecule ethylene glycol was confined. (a) Silica sodalite (SiO_2) has cubic cages with a lattice constant of 0.89 nm. The cages are connected by channels with a diameter of 0.28 nm. Just *one* molecule is confined to each cage. (b) Silicalite consists of pure SiO_2 and has a three-dimensional pore system with two different types of elliptical channel having cross sections of 0.56 nm $\times$ 0.53 nm and 0.55 nm $\times$ 0.51 nm. (c) Zeolite beta is an aluminosilicate with a three-dimensional pore system having pore diameters of 0.76 nm $\times$ 0.64 nm and 0.55 nm. (d) $AlPO_4$-5 is an aluminophosphate with one-dimensional channels (diameter 0.73 nm) arranged in a hexagonal array.

have channel-like pore systems (see figure 1). In silicalite-I, consisting of pure SiO_2, rings of ten Si and ten O atoms form a three-dimensional pore system with two types of elliptical channel having cross-sections of 0.56 nm × 0.53 nm and 0.55 nm × 0.51 nm [18]. In zeolite beta (a 12-ring system) the channels in [100] and [010] directions have diameters of 0.76 nm × 0.64 nm, whereas the channels in the [001] direction have smaller pores (0.55 nm × 0.55 nm) [19]. The Si:Al ratio of the sample was 40, to reduce the number of counter-cations in the channels. $AlPO_4$-5 has a one-dimensional pore system. In this aluminophosphate, the channels with diameters of 0.73 nm are arranged in a hexagonal array. To realize a larger pore diameter, sol–gel glass from Geltech Incorporated, USA, with specific pore sizes of 2.5 nm, 5.0 nm and 7.5 nm and a narrow pore size distribution was used.

Besides sodalite, which is already loaded with EG, after synthesis, all nanoporous hosts are heated to 330 °C with a temperature increase of 20 °C h^{-1} and evacuated at 10^{-5} mbar for 36 h to remove water and other volatile impurities. Afterwards the zeolitic host systems are filled with EG from the vapour phase in a closed vacuum chamber at 175 °C. The samples are cooled down to room temperature and remain in the vacuum chamber for 24 h before the dielectric measurements are carried out. The sol–gel glasses are disc shaped (diameter 10 mm, thickness 0.2 mm) and are filled from the liquid phase at 70 °C (with propylene glycol and salol). Some of the samples are chemically treated inside the closed vacuum chamber using hexamethyldisilazane (Aldrich Chemical Company) for 30 minutes at 70 °C and again evacuated for 3 h at 70 °C. This treatment replaces the –OH groups on the glass surface with trimethylsilyl groups. The replacement of the –OH groups is checked by means of FTIR spectroscopy and weighing; the surface density of trimethylsilyl groups decreases with decreasing pore size. Both sides of the sample discs are covered with aluminium foil (thickness 800 nm) to ensure a homogeneous field distribution and are mounted between gold-plated brass electrodes of the capacitor.

The dielectric measurements from 10^{-2} Hz to 10^7 Hz are carried out with a Solatron–Schlumberger frequency response analyser FRA 1260 in combination with a Novocontrol active sample cell BDC-S. The relative accuracy is ±5% in ϵ'; the resolution in $\tan\delta$ is better than 10^{-3}. For the frequency range 10^6–1.8×10^9 Hz a Hewlett Packard impedance analyser 4291A with a resolution in $\tan\delta$ better than 10^{-2} is employed. The sample temperatures are controlled in a nitrogen gas jet (Quatro, Novocontrol GmbH) with a stability better than ±0.05 K. Details of the set-up may be found in reference [20].

Isothermal data for the dielectric loss ϵ'' are fitted to a superposition of a relaxation function given by Havriliak and Negami (HN) and a conductivity contribution [21]

$$\epsilon'' = \frac{\sigma_0}{\epsilon_0}\frac{a}{\omega^s} - \mathrm{Im}\left[\frac{\Delta\epsilon}{(1 + (\mathrm{i}\omega\tau)^\alpha)^\gamma}\right]. \tag{1}$$

In this notation, ϵ_0 is the vacuum permittivity, σ_0 the DC conductivity and $\Delta\epsilon$ the dielectric strength. α and γ describe the symmetric and asymmetric broadening of the relaxation peak. The exponent s equals one for Ohmic behaviour, deviations ($s < 1$) are caused by electrode polarization or Maxwell–Wagner polarization effects and a is a factor having the dimension s^{1-s}. The accuracy in the determination of $\log_{10}\tau$ is $\leqslant$0.1 decades and of $\Delta\epsilon \leqslant 5\%$. Due to the fact that ϵ' and ϵ'' are connected by the Kramers–Kronig relations, a fit in ϵ' would not improve the limits of uncertainty. From the fits according to equation (1), the relaxation rate $1/\tau_{max}$ can be deduced, which is given at the frequency of maximum dielectric loss ϵ'' for a certain temperature. A second way to interpret the data is to use a relaxation time distribution of an ensemble of Debye relaxators with relaxation times τ and a distribution density $g(\tau)$. The imaginary part of the dielectric function is then represented by

$$\epsilon'' = \epsilon_\infty + (\epsilon_{st} - \epsilon_\infty)\int \frac{g(\tau)}{1 + \omega^2\tau^2}\,\mathrm{d}\tau \tag{2}$$

where ϵ_{st} and ϵ_∞ denote the low- and high-frequency values of the permittivity. $g(\tau)$ can be calculated analytically from the data [22] or extracted from the fit with HN functions [23]. To characterize the temperature dependence of the relaxation behaviour, an averaged relaxation time τ_{med} is used:

$$\tau_{med} = \langle \log \tau \rangle = \left(\int_{-\infty}^{+\infty} (\log \tau) g(\log \tau) \, \mathrm{d} \log \tau \right) \Big/ \left(\int_{-\infty}^{+\infty} g(\log \tau) \, \mathrm{d} \log \tau \right). \tag{3}$$

τ_{med} equals τ_{max} if the peak of a relaxation process is broadened only symmetrically. In general τ_{med} contains information about the low- and high-frequency side of a relaxation process whereas τ_{max} denotes only the position of the maximum loss. On the other hand, the calculation of τ_{med} can only be done with high accuracy if the dielectric strength is comparably strong. For that reason, τ_{max} is shown for molecules confined to zeolites and τ_{med} is calculated if the nanoporous sol–gel glasses are used.

Applying effective-medium theory, the relaxation rate may shift to higher frequencies. In the case of salol in sol–gel glasses, this effect is smaller than the limits of experimental accuracy. For propylene glycol in nanoporous sol–gel glasses, the shift can even be smaller than half a decade, depending on the dimensionality of the host system which is not exactly known. For ethylene glycol in $AlPO_4$-5, no effect is expected. In general, there is only in some special cases a shift in the relaxation rate, which is less than one decade. For a more detailed view, see reference [24].

To complete the information about the guest molecules in the zeolitic host systems, computer simulations are carried out to study the molecular arrangement of the molecules in the confining space. The molecular simulation program Cerius^2 is used on a Silicon Graphics workstation modelling a finite zeolite crystal of four unit cells surrounded by vacuum. By 'filling' the pores with EG, a completely loaded nanoporous host/guest system can be simulated and structural parameters like distance between molecules, density and length of H bonds can be determined. The simulations were carried out using three different force fields: the *dreiding* force field [25], the *Burchart universal* force field [26, 27] and the *consistent* force field cff 91. The three force fields provide the same results within statistical uncertainty.

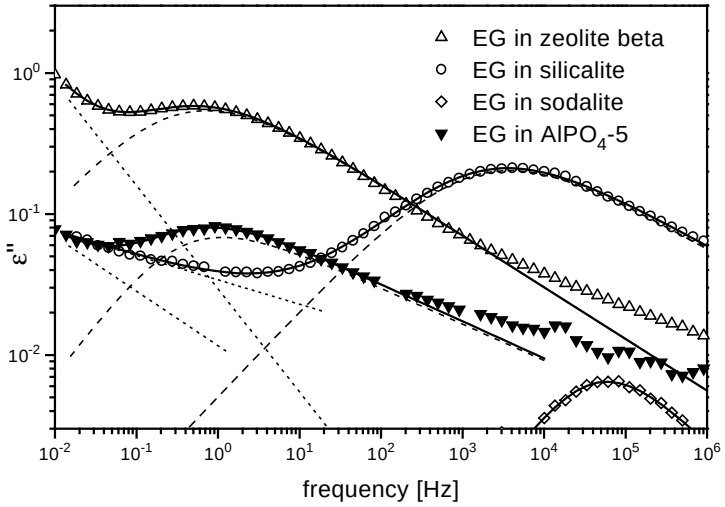

Figure 2. The dielectric loss ϵ'' versus frequency for ethylene glycol (EG) confined to zeolitic host systems as indicated. The solid curves are fits to the data (dotted curve: HN relaxation; dashed curve: the conductivity contribution).

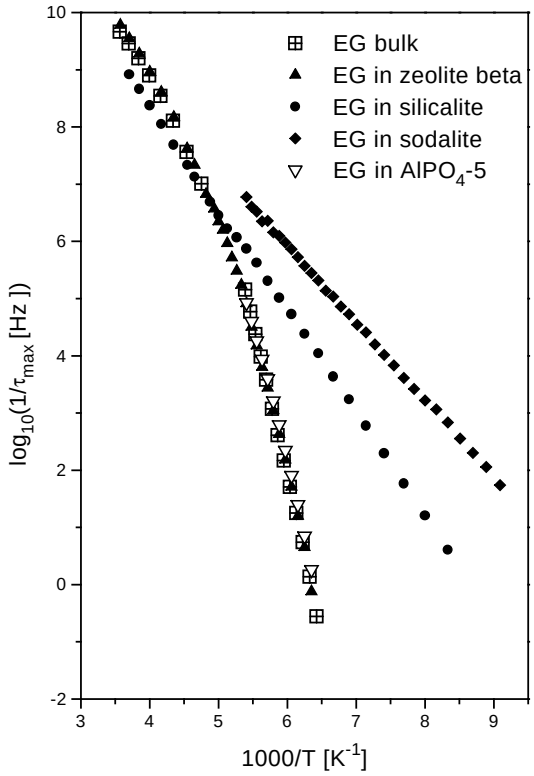

Figure 3. The relaxation rate versus inverse temperature for ethylene glycol confined to different zeolitic host systems as indicated. The errors are smaller than the sizes of the symbols.

3. Ethylene glycol in zeolites

Figure 2 shows the dielectric spectra for ethylene glycol (EG) confined to different zeolitic host systems at 160 K. The relaxation rates τ_{max} for EG in the zeolitic host systems differ by many orders of magnitude: in zeolites with smaller pores (silicalite and sodalite) the relaxation rates of EG are significantly faster compared to those for zeolite beta and $AlPO_4$-5. Especially for EG in sodalite, the relaxation strength is comparably weak. This is caused by EG molecules which are immobilized due to the interaction with the zeolitic host matrix. Figure 3 shows the logarithmic relaxation rate as a function of the inverse temperature for EG as bulk liquid and confined to zeolites. EG in zeolite beta (solid triangles) and in $AlPO_4$-5 (open triangles) has a relaxation rate like that for the bulk liquid (squares) following the characteristic Vogel–Fulcher–Tammann [28–30] temperature dependence (VFT dependence):

$$\frac{1}{\tau} = A \exp\left(\frac{DT_0}{T - T_0}\right) \tag{4}$$

where A is a prefactor, D the fragility parameter and T_0 the Vogel temperature. The relaxation rates of EG in silicalite and sodalite show Arrhenius-type temperature dependence.

The single-molecule relaxation of EG in sodalite is at $T \approx 155$ K faster by about six orders of magnitude than that for the bulk liquid. Its activation energy is 26 ± 1 kJ mol^{-1} and corresponds to the value for bulk EG at high frequencies and high temperatures (29 ± 2 kJ mol^{-1}) [31]. The relaxation process of EG in silicalite has a larger activation energy (35 ± 2 kJ mol^{-1})

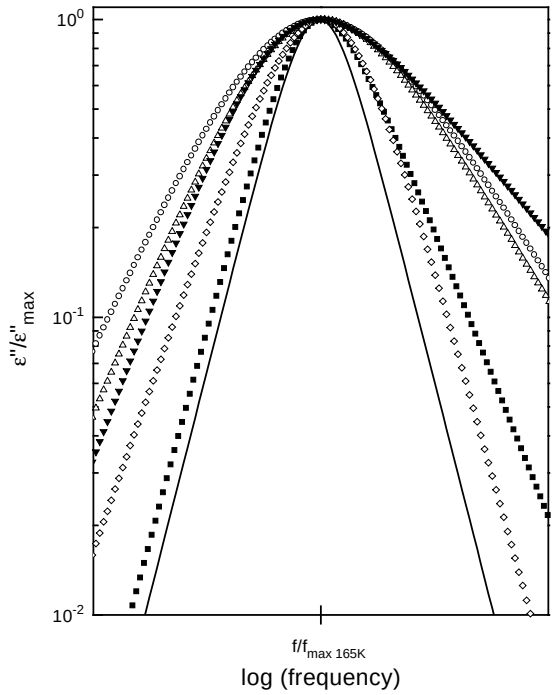

Figure 4. The normalized relaxation process for a Debye process (solid curve), for EG bulk (solid squares) and EG confined to zeolite beta (open triangles), silicalite (open circles), sodalite (open diamonds) and $AlPO_4$-5 (solid triangles) at 165 K. The curves are calculated from the HN-fit parameters.

which is still smaller than the apparent activation energy (the tangent to the VFT temperature dependence) of the bulk liquid. Its Arrhenius-like temperature dependence resembles the single-molecule relaxation of EG in sodalite.

Figure 4 shows the normalized relaxation peaks for all measured samples at 165 K calculated from the fits. Compared to a Debye process (solid curve), even the distributions for the bulk liquid and the single-molecule relaxation (EG in sodalite) are broadened. The distributions for EG in the other zeolitic host systems show very pronounced broadening at both low and high frequencies.

The computer simulations of EG in zeolitic host systems show that in silicalite the molecules are aligned almost in single file along the channels and that in zeolite beta and in $AlPO_4$-5 two EG molecules are located side by side in the channels. But neither for the distance between molecules nor for the average length of hydrogen bonds or for the density is a significant change found between the bulk liquid and the molecules in the restricting geometry.

However, for the number of neighbouring molecules (coordination number) a pronounced difference is observed (figure 5): the coordination number of 11 corresponds to the maximum value in the case of the random-close-packing model [32] and is found for the bulk liquid within a radius of $r = 0.66$ nm. EG in zeolite beta and in $AlPO_4$-5 has only five neighbouring molecules; hence one has to conclude that an ensemble as small as six molecules is sufficient for performing a liquid-like dynamics. As $AlPO_4$-5 has one-dimensional channels and no intersections between them, in contrast to zeolite beta, the dimensionality of the host system seems to play only a minor role as regards the dynamics of H-bonded guest molecules. Further

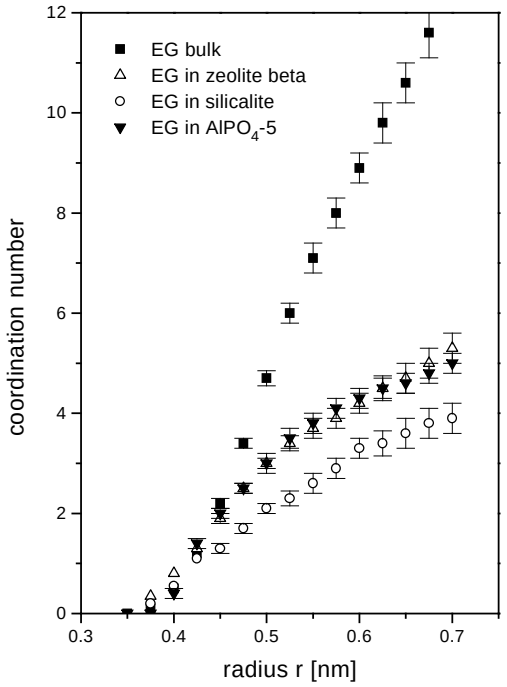

Figure 5. The average number of neighbouring molecules (coordination number) as a function of the radius of a surrounding sphere as calculated from the simulations for EG bulk liquid (squares) and EG confined to zeolite beta (solid triangles), to silicalite (circles) and to $AlPO_4$-5 (open triangles).

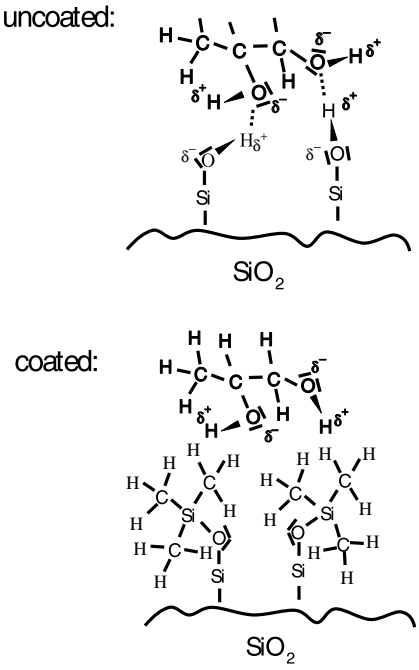

Figure 6. A schematic diagram of propylene glycol in the neighbourhood of an uncoated SiO_2 surface (top) and a silanized SiO_2 surface (bottom).

reduction in the channel size (as in the case of silicalite) decreases the average number of neighbouring molecules by about 1. This results in a sharp transition from a liquid-like dynamics to that of single molecules.

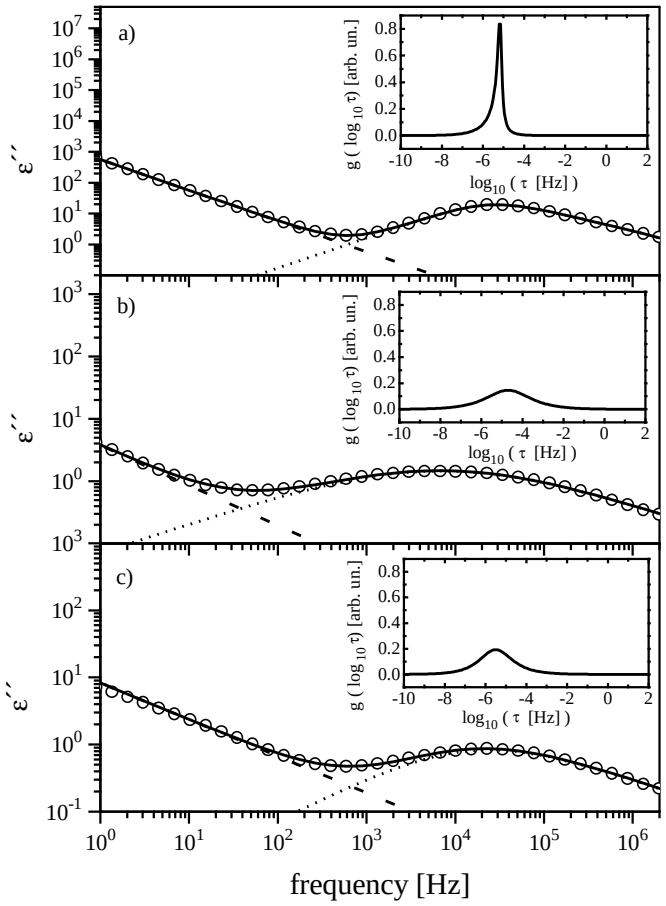

Figure 7. The dielectric loss of PG at a temperature $T = 210$ K. (a) Bulk PG, (b) PG confined to 2.5 nm uncoated pores, (c) PG confined to 2.5 nm coated pores. The error of the measured data (○) is smaller than the size of the symbols; solid curve: fit to the data (dotted curve: HN relaxation; dashed curve: the conductivity contribution). The insets show the resulting relaxation time distribution $g(\tau)$.

4. Propylene glycol in nanoporous sol–gel glasses

Propylene glycol (PG) is an H-bonded glass-forming liquid. Due to the fact that a freshly prepared SiO_2 surface (see the sample preparation section) is hydrophilic, one has to expect the PG molecules to form H bonds with the solid surfaces of the nanoporous system. This surface interaction can be counterbalanced by a silanization, as shown schematically in figure 6.

For PG in uncoated nanopores—compared to the bulk liquid—there is a pronounced broadening of the width of the dielectric loss curve and the relaxation time distribution function (figures 7(a), 7(b), figure 8). Silanization of the inner surfaces counteracts the broadening (figure 7(c), figure 8). The effect is—as expected—strongly temperature dependent and weakens with increasing thermal activation (figure 8): at a temperature of 185 K the low-frequency broadening of the relaxation time distribution function for PG in uncoated pores is completely removed and the mean relaxation time for PG in coated nanopores becomes even faster than that for the bulk. The broadening is interpreted as being caused by molecules close

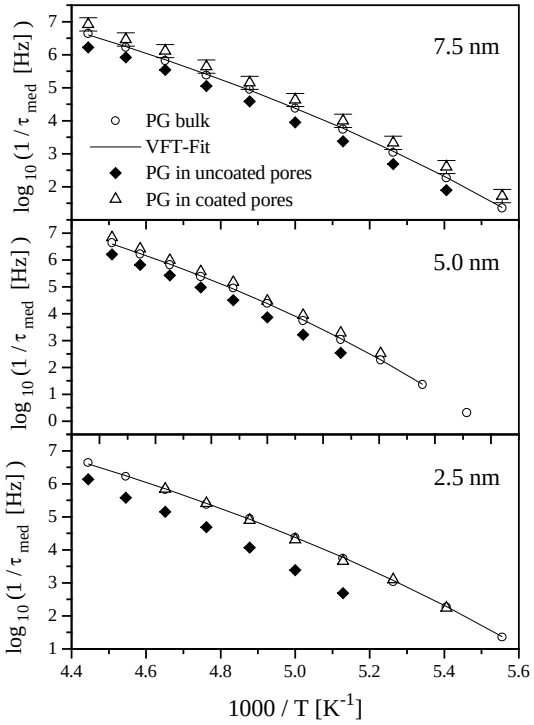

Figure 8. The mean relaxation rate of propylene glycol versus inverse temperature for the bulk liquid (open circles; solid curve: VFT fit) and for propylene glycol confined to uncoated (solid diamonds) and coated pores (open triangles) of different mean diameters of a sol–gel glass.

to the surface [6]. The lubrication hinders the formation of H bonds to the solid wall of the nanoporous ambience, hence decoupling its dynamics. For uncoated pores the opposite is true.

To characterize the temperature dependence of the relaxation rate, the averaged relaxation time τ_{med} is calculated as defined in equation (3). The temperature dependence follows for all (uncoated and coated) pores the well known VFT law (figure 9). The difference in relaxation rate for PG in uncoated and coated pores is maximal for the smallest pore size (2.5 nm) and lower temperature ($\approx$190 K). Despite the fact that due to the silane layer having a thickness of about 0.4 nm [8] the space for the PG molecules becomes even more confining, one finds a dynamics which is—within experimental accuracy—identical to that of the bulk liquid.

It is well known that for glass-forming liquids the product of the temperature T and dielectric strength $\Delta\epsilon$ increases with decreasing temperature [33] (for a simple Debye relaxation it should be constant, neglecting density effects). This effect vanishes for the dynamic glass transition if it takes place in the nanoporous systems (figure 10). The fact that the dielectric strength becomes smaller with decreasing pore diameter is attributed to the change in the surface-to-volume ratio of the nanoporous system.

In summary, one has to conclude that the dynamics of the H-bonded model system propylene glycol depends strongly on the surface treatment of the nanopores. In freshly prepared uncoated pores, the relaxation rate of the glass-forming system is smaller as compared to that for the bulk liquid and the relaxation time distribution function is strongly broadened on the low-frequency wing. Silanization of the inner surfaces decouples the dynamics of the confined liquid from the solid wall and makes the relaxation rate in 7.5 nm pores even

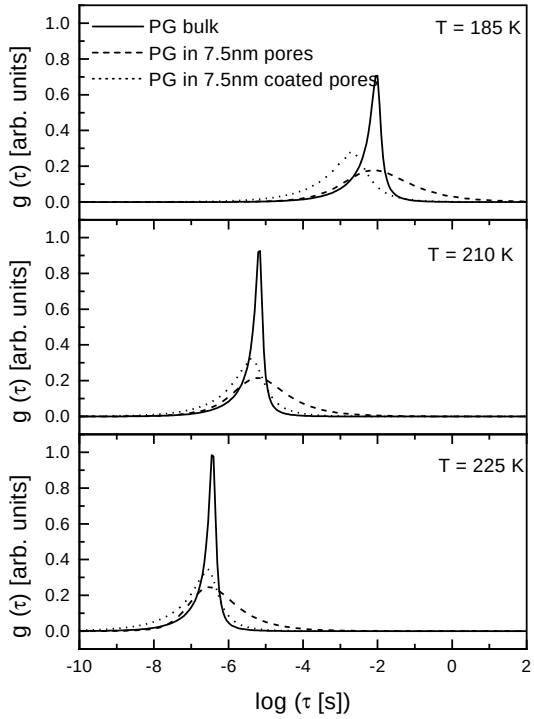

Figure 9. The relaxation time distribution function versus relaxation time for propylene glycol as a bulk liquid (solid curve), in uncoated pores (dashed curve) and in coated pores (dotted curve) at different temperatures.

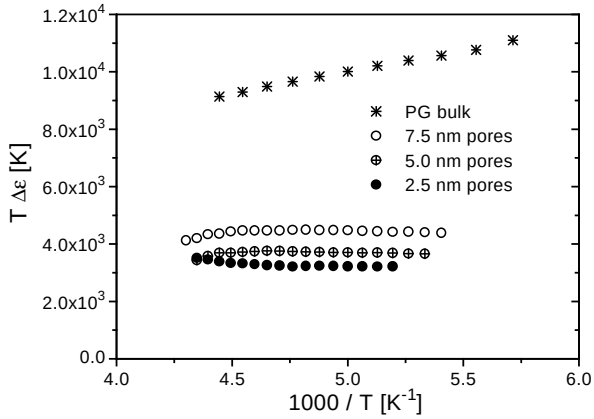

Figure 10. The dielectric strength $\Delta\epsilon$ times temperature T versus inverse temperature for propylene glycol as a bulk liquid ($*$) and confined to silanized pores of a sol–gel glass having different diameters of 7.5 nm ($\bigcirc$), 5.0 nm ($\oplus$) and 2.5 nm ($\bullet$).

faster than in the bulk. From the size of the pores one has to conclude that the molecular rearrangements of PG take place on a length scale of $\leqslant$1.5 nm.

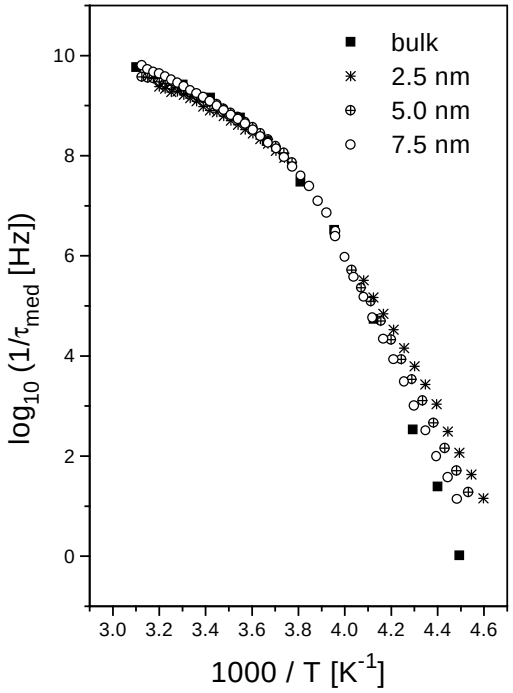

Figure 11. The mean relaxation rate versus inverse temperature of salol as bulk liquid (solid squares) and confined to silanized pores of sol–gel glass having different mean diameters.

5. Molecular dynamics of salol in lubricated nanoporous sol–gel glasses

The molecular dynamics of the glass transition of the 'quasi'-van der Waals liquid salol confined to nanopores (2.5, 5.0 and 7.5 nm) with lubricated inner surfaces is found to be faster (by up to two orders of magnitude) than in the bulk liquid (figure 11 [8]). This effect observed by broad-band dielectric spectroscopy is also supported by calorimetric measurements, where the largest shift of the glass transition to lower temperatures is found for the smallest pores. The question arises of whether this confinement effect is caused by a pore-size-dependent decrease of the density of the confined liquid.

It can be assumed that the mean relaxation rate $1/\tau$ obeys a VFT law where the Vogel temperature varies with the pore size in a similar way to the measured calorimetric glass transition temperature (figure 12(a)). Then the derivative $\mathrm{d}(\log(1/\tau))/\mathrm{d}(1000/T)$ delivers a temperature dependence as shown in figure 12(b). This can be compared with the difference quotient as determined experimentally from the relaxation rate measured in temperature steps of 0.5 K (figure 12(c)). It turns out that the experimentally deduced difference quotient behaves qualitatively differently as regards its temperature dependence compared to the calculated differential quotient in figure 12(b). In the temperature interval between 333 K and 260 K, the apparent activation energies for the bulk and the confined (2.5 and 7.5 nm) liquid coincide within experimental accuracy. But for lower temperatures, suddenly the charts bend off; this takes place for the 2.5 nm pores at 256 ± 3 K and for 7.5 nm pores at 245 K $\pm$ 3 K. The temperature dependence is in sharp contrast to the results (figure 12(b)) which one would expect from a dependence like that displayed in figure 12(a), assuming a slowly varying temperature dependence of the density. Hence one has to conclude that the experimental observations cannot

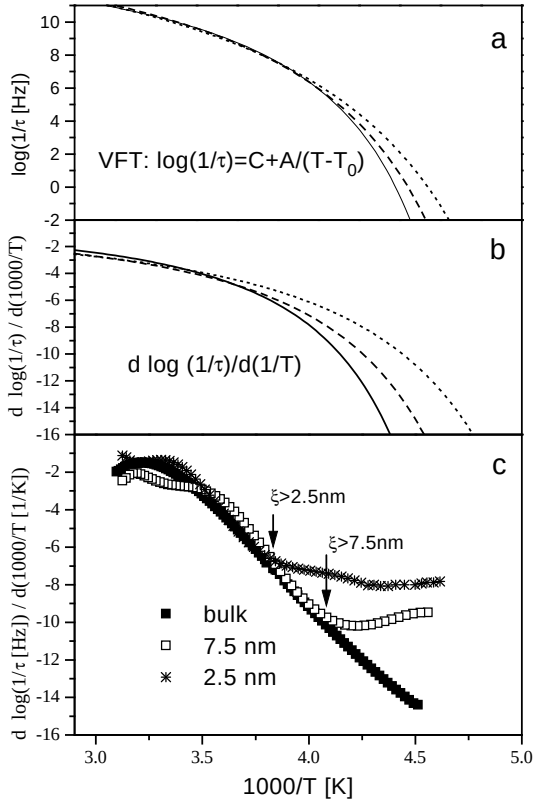

Figure 12. (a) The calculated dependence of the mean relaxation rate versus inverse temperature assuming a VFT law, where T_0 is shifted according to the calorimetrically measured shift of T_g. Solid curve: bulk liquid, $T_g = 222$ K; dashed curve: salol confined to a silanized sol–gel glass having a mean diameter of 7.5 nm, $T_g = 214$ K; dotted curve: salol confined to a silanized sol–gel glass having a mean diameter of 2.5 nm, $T_g = 207$ K. (b) The calculated derivative of $\log(1/\tau$ (Hz)) versus inverse temperature assuming the temperature dependence shown in (a). The units are omitted for reasons of space. They are the same as in part (c) of this figure. (c) The experimentally determined difference quotient $\Delta(\log(1/\tau$ (Hz)))$/\Delta(1000/T$ (K)) for the data shown in figure 11 for the bulk liquid (■), salol confined to silanized nanopores of 7.5 nm (□) and salol confined to silanized nanopores of 2.5 nm (∗).

be explained on the basis of such a density argument. Instead it is suggested that the measured confinement effects are caused by the cooperative nature of the dynamic glass transition. With decreasing temperature the size of cooperatively rearranging domains is growing and the apparent activation energy increases. If, due to the confinement of the nanoporous system, further growth is prohibited, the VFT dependence turns very suddenly into an Arrhenius-like type of thermal activation.

6. Conclusions

The question ‘how many molecules form a liquid’ does not have a general answer: for ethylene glycol confined to zeolites of varying size and topology, one can show that a sharp transition exists from a single-molecule-like relaxation with an Arrhenius temperature dependence to a liquid-like dynamics obeying a Vogel–Fulcher–Tammann law. An ensemble of five molecules

performs a single-molecule dynamics while six molecules are already sufficient to show a dynamics which is identical in its mean relaxation rate to that of a bulk liquid.

The experiments on (coated and uncoated) nanopores do not allow us to draw such clear-cut conclusions, because the nanoporous system is less well defined as compared to zeolites: neither the topology nor the distribution of pore sizes is very well known. These drawbacks do not prevent us from coming to the conclusion that the relaxation of propylene glycol (PG) takes place on a length scale smaller than 1.5 nm.

For the 'quasi'-van der Waals liquid salol, one finds a very different behaviour compared to that of the H-bond-forming liquids like ethylene and propylene glycol. In lubricated nanopores, salol shows no surface-dominated relaxation process; instead, one observes over a wide temperature range a dynamics fully comparable to that of a bulk liquid. But with decreasing temperature, suddenly the VFT temperature dependence turns into an Arrhenius-type dependence. This transition depends strongly on the pore diameter and enables one to deduce the length scale on which cooperative rearrangements in salol take place. It is shown that the confinement effect cannot be caused by the temperature dependence of the density of the confined liquid.

Acknowledgments

Support by the Deutsche Forschungsgemeinschaft within the 'SFB 294' and the Schwerpunktprogramm 'Nanostrukturierte Wirt/Gast-Systeme' is gratefully acknowledged.

References

[1] Böhmer R, Ngai K L, Angell C A and Plazek D J 1993 *J. Chem. Phys.* **99** 4201
[2] Hansen J-P 1990 *Theory of Simple Liquids* 2nd edn (London: Academic)
[3] Johari G P 1984 *Relaxations in Complex Systems* ed K L Ngai and G B Wright (Washington, DC: ONA) p 17 ff
[4] Donth E 1981 *Glasübergang* (Berlin: Akademie)
[5] Götze W 1991 *Liquids, Freezing and Glass Transition* ed D Levesque, Hansen J-P and J Zinn-Justin (Amsterdam: North-Holland)
[6] Gorbatschow W, Arndt M, Stannarius R and Kremer F 1996 *Europhys. Lett.* **35** 719
[7] Arndt M, Stannarius R, Gorbatschow W and Kremer F 1996 *Phys. Rev.* E **54** 5377
[8] Arndt M, Stannarius R, Groothues H, Hempel E and Kremer F 1997 *Phys. Rev. Lett.* **79** 2077
[9] Aliev F M 1996 *Liquid Crystals in Complex Geometries* ed G P Crawford and S Žumer (London: Taylor and Francis) ch 17
[10] Adam G and Gibbs J H 1965 *J. Chem. Phys.* **43** 139
[11] Ngai K L 1993 *Disorder Effects on Relaxational Processes* ed R Richert and A Blumen (Berlin: Springer) p 89 ff
[12] Williams G and Fournier J 1996 *J. Chem. Phys.* **184** 5690
[13] Sappelt D and Jäckle J 1993 *J. Phys. A: Math. Gen.* **26** 7325
[14] Fischer E W, Donth E and Steffen W 1992 *Phys. Rev. Lett.* **68** 2344
[15] Fischer E W 1993 *Physica* A **201** 183
[16] Bibby D M and Dale M P 1985 *Nature* **317** 157
[17] Braunbarth C M, Behrens P, Felsche J and van de Goor G 1997 *Solid State Ion.* **101–103** 1273
[18] Meier W M, Olson D H and Baerlocher C 1996 *Atlas of Zeolite Structure Types* (Amsterdam: Elsevier)
[19] Newsam J M, Treacy M M J, Koetsier W T and de Gruyter C B 1988 *Proc. R. Soc.* **420** 375
[20] Kremer F, Boese D, Maier G and Fischer E W 1989 *Prog. Polym. Sci.* **80** 129
[21] Havriliak S and Negami S 1966 *J. Polym. Sci.* C **14** 99
[22] Schäfer H, Sternin E, Stannarius R, Arndt M and Kremer F 1996 *Phys. Rev. Lett.* **76** 2177
[23] Nozaki R and Mashimo S 1987 *J. Chem. Phys.* **87** 2271
[24] Pelster R 1999 *Phys. Rev.* B at press
[25] Mayo S L, Olafson B D and Goddard W A III 1990 *J. Phys. Chem.* **94** 8897
[26] Rappe A K, Casewit C J, Colwell K S, Goddard W A III and Skiff W M 1992 *J. Am. Chem. Soc.* **114** 10 024
[27] Burchart E 1992 *Thesis* Technische Universiteit Delft

[28] Vogel H 1921 *Phys. Z.* **22** 645
[29] Fulcher G S 1925 *J. Am. Chem. Soc.* **8** 339
[30] Tammann G and Hesse G 1926 *Anorg. Allg. Chem.* **156** 245
[31] Jordan B P, Sheppard R J and Szwarnowski S 1978 *J. Phys. D: Appl. Phys.* **11** 695
[32] Cusack N E 1987 *The Physics of Structurally Disordered Matter* (Bristol: Hilger)
[33] Schönhals A, Kremer F, Hofmann A, Fischer E W and Schlosser E 1993 *Phys. Rev. Lett.* **70** 3459